THE ASTROPHYSICAL JOURNAL, 250:55–65, 1981 November 1

EMPIRICAL RESULTS FROM A STUDY OF ACTIVE GALACTIC NUCLEI[1]

JAMES M. SHUDER AND DONALD E. OSTERBROCK
Lick Observatory, Board of Studies in Astronomy and Astrophysics, University of California, Santa Cruz
Received 1981 March 6; accepted 1981 May 4

ABSTRACT

Spectrophotometric observations are presented for emission-line galaxies. When combined with previous Lick Observatory measurements, they are used to deduce criteria that allow the Seyfert 2 phenomena to be quantitatively isolated from the narrow-emission-line galaxies. These criteria are based on our finding that galaxies with [O III] λ5007/Hβ < 3 have emission line widths that are usually considerably smaller than the widths in galaxies with [O III] λ5007/Hβ > 3. In addition, large He II λ4686/Hβ ratios are consistent with [O III] λ5007/Hβ > 3. We also compare the physical conditions in the narrow-line regions of Seyfert 1 galaxies with those in Seyfert 2 galaxies. Significant differences are found for the temperature-sensitive [O III] ratio, and for the luminosity of [Fe VII] λ6087 relative to the luminosity of the low-ionization forbidden lines.

Subject headings: galaxies: nuclei — galaxies: Seyfert — spectrophotometry

I. INTRODUCTION

A spectroscopic survey of galaxies suspected or known to have emission lines has been under way for some time at Lick Observatory. Seyfert galaxies were originally defined as objects with many "high-excitation" emission lines, similar to those in planetary nebulae, in their spectra (Seyfert 1943). From the first, it was clear that galaxies isolated in this way have unusually luminous stellar or semistellar nuclei, and that their emission lines are characteristically broader than those in the spectra of typical emission-line galaxies. Much additional observational research since Seyfert's original paper has shown that broad emission lines, a wide range of ionization, and bright nuclei are all very well correlated with one another (see, e.g., Weedman 1977). Seyfert galaxies may be classified into two well defined types on the basis of the widths of their emission-line profiles, Seyfert 2 galaxies being those with narrower H I, He I, and He II lines, but still broad in comparison with typical emission-line galaxies (Khachikian and Weedman 1971, 1974).

In an earlier analysis of objects from the Lick survey, Koski (1978) reported that the Seyfert 2 galaxies form a distinct group, but with fuzzy edges. He suggested that the Seyfert 2 phenomenon refers only to objects with average full width at half-maximum (FWHM) of about 500–600 km s^{-1}, and with strong emission lines of high ionization, such as [O III], [Ne V], and He II. More recently, Heckman, Balick, and Crane (1980) and Baldwin, Phillips, and Terlevich (1981) used only line ratios to try to distinguish Seyfert 2 galaxies from H II region–like galaxies and to distinguish between energy-input mechanisms.

The purpose of the present paper is to present additional spectroscopic measurements of Seyfert 2 and emission-line galaxies which, when compared with other Lick Observatory measurements, provide a large homogeneous set of data for these objects. Convenient criteria are also suggested for classifying galaxies from their spectra as Seyfert 2 galaxies or as narrow emission-line galaxies that are not members of this class. In addition, quantitative comparisons are drawn between the physical conditions in the narrow-line regions of Seyfert 1 galaxies and those in Seyfert 2 galaxies.

II. OBSERVATIONS

The objects reported on here were observed during the years 1975–1980 with the image-tube image-dissector spectrograph (Miller, Robinson, and Wampler 1976) at the Cassegrain focus of the 3 m Shane telescope at Lick Observatory. Primarily, low-dispersion scans were obtained, giving an instrumental resolution at FWHM of about 10 Å and a wavelength coverage of approximately 2500 Å. In most instances two overlapping regions were observed to cover the range $\lambda\lambda$3500–7000, with a considerable range in common around Hβ and [O III] $\lambda\lambda$4959, 5007. For a few objects, high-dispersion scans were obtained covering half the range of the low-dispersion scans at a resolution of about 5 Å. In all cases the entrance aperture of about 2".7 × 4" was centered on the nucelus of the galaxy.

The observations were reduced to a linear wavelength scale by using laboratory wavelengths of comparison lamps, and calibrated into energy units by comparison with standard stars (Stone 1974, 1977), on the system of Hayes and Latham (1975). The reduced scans were then measured using standard Lick Observatory programs as outlined by Koski (1976), Costero and Osterbrock (1977), and Osterbrock (1977).

III. RESULTS

The galaxies in this survey exhibit a wide range of spectral appearances. For example, NGC 5005 has a

[1] *Lick Observatory Bulletin*, No. **888**.

rather low level of ionization, as indicated by the presence of only Hα, [N II], [S II], [O II] emission lines and, at a fainter level, [O III]. This contrasts with UM 16, which has a higher level of ionization as evidenced by strong [O III], He II, [Ne III], and [Fe VII]. Both of these sources have absorption lines characteristic of integrated late-type stellar spectra. Only six of 17 objects for which the blue and red spectral regions were observed, showed any amount of H I absorption (Mrk 463 W, Mrk 622, Mrk 739, Mrk 1158, Akn 160, and Kaz 26). (The coordinates and finding chart for Kaz 26 can be found in Kazarian 1979, while the coordinates and finding charts for the UM objects can be found in MacAlpine, Lewis, and Smith 1977; MacAlpine, Smith, and Lewis 1977*a*; and MacAlpine, Smith, and Lewis 1977*b*.) Table 1 gives the measured absorption-line equivalent widths (with probable errors of about ±20%) for all of the objects, in their own rest systems.

a) Emission-Line Ratios

The galaxies were measured by a procedure described by Koski (1976) which corrects for the stellar absorption lines in their spectra. The galaxies used for continuum and absorption-line removal were either NGC 6482 and NGC 6702, which are ellipticals with form classes E3 and E2 and integrated spectral types G0 and G3, respectively, or NGC 2681, an Sa galaxy of integrated spectral type F8 (Humason, Mayall, and Sandage 1956). Since it is uncertain whether or not this technique is correct (because of possible reddening corrections or imperfect matches to the intrinsic galaxy), the line fluxes were obtained from the original unsubtracted scans and averaged with those obtained from the subtracted scans. The resulting average values are listed in Table 2 relative to [O III] λ5007, whose flux is also given, as well as the continuum flux at λ4800.

TABLE 1

ABSORPTION-LINE EQUIVALENT WIDTHS (Å)

Object	Ca II K	G-band	Mg I *b*	Na I D
MCG 6-30-15	12	8.2:	4.2	3.1
Akn 347	9.1	6.9	3.4	3.0
UM 16	7.3	4.8	1.8	1.3
Mrk 533	4.9:	2.1	1.9	1.0
NGC 6251	7.2	5.4	4.2	5.3
I Zw 92	1.6:	1.6:	1.0	0.9:
Mrk 612	4.6	3.0	3.6	2.8
Mrk 463 E	2.9	1.3	1.2	2.0:
Mrk 622	2.7	3.0	1.9	1.3
Mrk 463 W	3.6	1.6	1.9	2.4
M81	9.3	5.5	5.1	6.0
Mrk 833	4.1	2.6	2.8	1.2
NGC 5005	8.3	2.5	3.8	6.0
Mrk 1158	1.3	1.6	1.8	0.5:
UM 213			2.1	1.8
Akn 160	4.5	1.6	2.9	2.5
Mrk 739	5.9	3.9	3.4	1.7
Kaz 26	0.9	1.1	1.0	1.3
UM 71			2.3	2.0
UM 60			3.2	2.3
Akn 179			5.0	2.7
Akn 145			2.3	2.5

The measured redshift in the rest system of the Sun is also listed for each galaxy. [O III] λ5007 was chosen as the fiducial line since Hβ is often weak and can be greatly affected by the removal of the stellar spectrum. For two objects, Akn 179 and Akn 145, [O III] λ5007 and Hβ are so weak that Hα was used as the standard line.

In addition to the underlying absorption, the accuracy of the line-flux measurements is affected by blending with nearby lines. For these cases ([S II] λλ6716, 6730, Hα with [N II] λλ6548, 6583, Hγ with [O III] λ4363, [S II] λλ4068, 4076 with Hδ, and [Ne III] λ3869 with He I + H8 λ3889), the flux of the entire blend was measured and then decomposed as described by Phillips (1978) to obtain the individual fluxes.

The probable errors in the line ratios are approximately ±10% for the stronger lines, and ±20% for weak lines. Very weak lines are denoted by either a colon, symbolizing a probable error of a factor of about 2, or an upper limit symbol. These large errors probably result from the underlying absorption-line spectrum and blending effects. The absolute-flux measurements have probable errors of about ±35%, judging from differences in our blue and red scans. The large errors result largely from the fact that the standard stars are observed only at the beginning and ending of the night, so that any variations in seeing or transparency enter directly into the absolute values of the flux.

Comparison of line ratios for I Zw 92 with those reported by O'Connell and Kingham (1978) shows excellent agreement, with the differences well within the quoted errors. The same situation also applies for the Hβ fluxes, which agree within the uncertainties of the measurements. The contrary is the case when a comparison of the same object is made with the measurements published by Kunth and Sargent (1979). In this case the average difference in the line-ratio measurements is 20%, contrasted with an average difference of 13% in the previous example. Furthermore, the Hβ fluxes differ by a factor of about 2. The cause of these discrepancies is unknown, but may result from the greatly different entrance apertures used in the two sets of observations.

Two other comparisons can be made, one with M81 and one with NGC 6251. For M81, Peimbert and Torres-Peimbert's (1981) measurements are in fair agreement with the present results, considering the large stellar absorption-line spectrum present in this galaxy. Their measured ratio of the strength of the Hα, [N II] blend with respect to λ5007 differs by a factor of about 2 from our measurement. This difference most likely arises from the corrections applied for the stellar absorption lines. In addition, separating the broad and narrow components of the Hα complex from the [N II] lines shows individual differences. For instance, the present paper reports a ratio of the intensities of the broad and the narrow component of Hα to be about 1.5, while Peimbert and Torres-Peimbert find it to be 3.9. At the same time, the measured ratio of the total Hα + [N II] flux to that of [S II] λλ6716, 6730, differs by only 18%. For NGC 6251, Miley and Osterbrock (1979) report line ratios that differ significantly from those of the present work. The

disparity can be attributed to the difference between the technique of averaging measurements of the original scan with those of the subtracted scan (corrected for stellar absorption lines), as in this survey, and the technique of reporting only the line ratios of the subtracted scan, as Miley and Osterbrock (1979) did.

b) *Reddening*

All of the galaxies reported in detail here have a Balmer decrement that is steeper than the decrement expected from pure recombination. If this difference is due entirely to extinction by dust, then the observed Balmer-line ratios can yield the amount of reddening, E_{B-V}, when compared to the theoretical ratios calculated by Brocklehurst (1971). The exact procedure used to determine the reddening is described by Koski (1976, 1978). Briefly, a least-squares fit is performed between the observed and predicted case B decrements, using the reddening curve parametrized by Miller and Mathews (1972). In general, three Balmer lines were used, although in some cases (NGC 5005 or Akn 179, for example) only Hα and Hβ, could be used, and in other cases (UM or I Zw 92 for example) Hα, Hβ, Hγ, and Hδ could be employed in this fitting procedure. The extinctions E_{B-V} determined in this way are given in Table 3 and range from 0.26 to 1.7 (with the exception of Akn 145).

For I Zw 92, in which an ultraviolet scan was obtained, the amount of extinction could also be measured by comparing the observed ratio of He II λ3204/He II λ4686 to that predicted by Seaton (1978). For a temperature of 20,000 K and a density of 10^4 cm^{-3}, $E_{B-V} = 0.37 \pm 0.10$ is obtained using the extinction curve of Miller and Mathews (1972), which agrees favorably with that determined by the Balmer lines. Similarly, the He II ratio can be applied in UM 16 and Akn 347. Although the He II λ3204 line is not determined with high accuracy in these cases, it nevertheless can be used to yield an independent check on the reddening. For similar assumptions, extinctions $E_{B-V} = 0.5$ and 0.2, respectively, are indicated. While these values do have large errors, they are at least consistent with some amount of extinction as determined by the H I Balmer lines.

c) *Physical Conditions*

The amounts of extinction given in Table 3 were removed from the measured line ratios, and the corrected ratios, $I(\lambda)/I(5007)$ also listed in the same table. Using standard nebular diagnostics, these intrinsic ratios can then yield some insights into the physical conditions of these objects. Listed in Table 4 are the O^{++} temperatures, as determined from I([O III] λ4959 + [O III] λ5007)/I([O III] λ4363), for the low-density limit, using the collision strengths given by Seaton (1975). In general, these temperatures range from about 10,000 K to 22,000 K. Also given in Table 4 are the electron density, and in some instances the temperature, in the S^+–N^+ region. Where this temperature could not be determined from either the [N II] line ratio $I(\lambda6548 + \lambda6583)/I(\lambda5755)$ or the [S II] line ratio $I(\lambda6716 + \lambda6730)/(I(\lambda4068 + \lambda4076)$, the density is given at a temperature of 10^4 K (or the O^{++} temperature if it is lower than 10^4 K). The range in temperature in the N^+–S^+ zone is from about 6000 K to 15,000 K, while the electron density ranges from the low density limit up to about 2000 cm^{-3}.

d) *Line Widths*

The FWHM of the emission lines range from less than 150 km s^{-1} to about 800 km s^{-1}. The values listed in Table 5 are averages of the stronger lines and have probable errors of about $\pm 30\%$. These results were obtained by convolving a comparison line with a Gaussian profile and comparing the resulting profile with the observed line. A comparison line was selected whose position on the image tube was very nearly the same as that of the observed line. This technique avoids any distortion effects across the tube. This measurement procedure, as Koski (1976) showed, proved sensitive to the measurement of widths somewhat below the resolution limit of the scans.

For the most part, the line profiles are symmetric and well represented by a Gaussian profile from the peak intensity, down to 0.25 of the peak intensity; below this level the observed line profiles appear to be broader than a Gaussian. However, several galaxies display peculiar profiles, which can be classified into three groups: those with blue wings, those with multiple components clearly visible, and those with a broad Hα component. These groups are discussed separately below.

Blue wings.—Mrk 533 has very noticeable blueward wings on all of the emission lines (as originally suggested by Afanas'ev *et al.* 1980). Except [S II] $\lambda\lambda$6716, 6730 and possibly [O II] λ3727. The extent of this emission compared to the redward emission is about 20% larger at the half-intensity level (300 km s^{-1} compared to 250 km s^{-1}) and a factor of about 2 larger at the zero-intensity level (1950 km s^{-1} compared to 900 km s^{-1}). It is interesting to note that in Mrk 533 the half-width at zero intensity (HWZI) of the symmetric [S II] lines (= 825 km s^{-1} for both the blue and red sides) is comparable to the redward extent of the other emission lines. An interpretation involving a high-density blueshifted gaseous component would be straightforward if it were not for the suggestion of the wing on [O II] λ3727. Certainly, future observations are required to resolve this problem. However, some insight into the physical conditions of this blueshifted gas can be gained by using the [S II] lines to deblend the profiles of the other emission lines into a symmetric component plus a blueshifted component. Examining the [O III] λ5007 and Hβ lines in this manner yields an [O III]/Hβ ratio of about 25 for the blueward gas and a ratio of about 10 for the deblended profiles. For [O I]/Hβ, the blueward gas has a ratio of 0.33, while the symmetric profiles indicate a ratio of 0.4. These results, while not highly accurate, are suggestive of a higher level of ionization for the gas that is blueshifted relative to the peak of the emission lines.

Two other examples of this blueward asymmetry are found in Mrk 463E and I Zw 92. For Mrk 463E the blue half-width at half-maximum (HWHM) is about 10–15%

TABLE 2

EMISSION-LINE FLUX RATIOS

Line	MCG 6-30-15	Akn 347	UM 16	Mrk 533	NGC 6251	I Zw 92	Mrk 612	Mrk 463 E	Mrk 622	Mrk 463 W	M 81
O III λ3133		0.017:	...			0.009					
He II λ3204		0.007:	0.006:			0.004					
[Ne V] λ3346		0.022	0.018			0.020					
[Ne V] λ3426		0.068	0.049			0.058					
O III λ3444		≤0.002	0.010			0.003			0.16		
[O II] λ3727	≤0.31	0.10	0.13	0.084	0.030:	0.20	0.11	0.21	0.49	0.40	1.40
[Ne III] λ3869	≤0.071	0.055	0.081	0.076	...	0.097	0.059	0.065	0.064	0.053	0.180:
He I + H8 λ3889	...	0.012	0.013	0.010	...	0.017	0.008	0.013	...	0.013	...
[Ne III] λ3967	...	0.010	0.026	0.023	...	0.034	0.012	0.025	...	0.003	≤0.029
[S II] λ4071	≤0.005	0.006:	0.008	0.010	...	0.020	0.004	0.016	≤0.018	0.005:	≤0.18
Hδ	...	0.008:	0.012	0.008	...	0.019	0.007	0.018	...	0.007:	≤0.038
Hγ	0.008:	0.026	0.025	0.025	≤0.019	0.046	0.035	0.041	0.015:	0.042	≤0.081
[O III] λ4363	≤0.008	0.020	0.013	0.009	≤0.053	0.030	0.015	0.013	0.004	≤0.019	...
He II λ4686	≤0.053	0.019	0.024	0.022	...	0.014	0.027	0.015	0.026	0.034	...
Hβ	0.051:	0.062	0.068	0.078	0.082:	0.096	0.10	0.13	0.16	0.20	0.31
[O III] λ4959	0.27	0.33	0.32	0.32	0.30	0.35	0.31	0.33	0.33	0.28	0.40
[O III] λ5007	1.00	1.00	1.00	1.00	1.00	1.00	1.00	1.00	1.00	1.00	1.00
[Fe VII] λ5159	...	≤0.003	0.010	0.002	...	0.003	≤0.004	≤0.003	≤0.004	...	...
[N I] λ5199	0.022:	0.005:	0.005	0.004:	0.032:	0.002	0.012	0.012	0.022	0.034:	0.070:
[Ca V] λ5309	...	0.007:	0.001	≤0.001	...	0.001	0.003	0.004:	...	0.004:	...
[Fe VII] λ5721	...	0.011	0.006	0.004	...	0.004	≤0.004	...	≤0.008	...	...
[N II] λ5755	0.022:	≤0.003	≤0.001	0.001	0.035	0.002	0.007	≤0.001	≤0.003	...	≤0.012
He I λ5876	0.059	0.011	0.018	0.014	0.008:	0.010	0.032	0.015	0.019	0.017	≤0.057
[Fe VII] λ6087	≤0.003	0.014	0.017	0.009	...	0.008	≤0.003	0.003:	≤0.010	...	...
[O I] λ6300	0.114	0.038	0.029	0.030	0.29	0.061	0.040	0.055	0.12	0.060	1.14
[S III] λ6312	...	...	...	...	...	...	0.006	...	0.033	0.019	...
[O I] λ6364	0.054:	0.007:	0.009	0.014	0.053	0.015	0.008	0.020	0.041	0.012	0.29
[Fe X] λ6374	...	...	...		...	≤0.002	...	...	...	...	...
[N II] λ6548	0.41	0.16	0.070	0.12	1.11	0.044	0.25	0.071	0.59	0.21	1.51
Hα	0.78	0.37	0.32	0.36	1.24	0.36	0.55	0.48	1.88	1.16	2.34 N[a]
											3.49 B[a]
[N II] λ6583	1.24	0.45	0.20	0.36	3.31	0.13	0.74	0.23	1.77	0.62	4.32
[S II] λ6716	0.34	0.11	0.056	0.054	0.18	0.053	0.16	0.098	0.32	0.25	0.90
[S II] λ6730	0.33	0.11	0.057	0.063	0.20	0.058	0.12	0.090	0.35	0.21	1.08
F λ5007[b]	3.6(−15)	1.3(−13)	2.5(−13)	4.9(−13)	5.2(−15)	9.7(−13)	1.8(−13)	3.7(−13)	2.9(−14)	2.5(−14)	9.2(−14)
F λ4800[c]	2.6(−27)	1.2(−26)	6.7(−27)	8.8(−27)	1.4(−26)	1.1(−26)	1.5(−26)	4.7(−27)	1.6(−26)	5.3(−27)	2.8(−25)
z	0.05699	0.02286	0.05788	0.02873	0.02433	0.03750	0.02022	0.05006	0.02283	0.05060	0.00039

[a]Separate measurements for broad and narrow components.
[b]erg s^{-1} cm^{-2}.
[c]erg s^{-1} cm^{-2} Hz^{-1}.

larger than the red HWHM, while the blue HWZI is about 50–60% larger than the red HWZI. For I Zw 92 the asymmetry is even weaker, with the blue HWZI being only about 30% larger than the red HWZI. Because of the weakness of these components no separation was possible as it was in the case of Mrk 533.

Multiple components.—Two galaxies fall into this group—Mrk 622 and NGC 5005. Mrk 622 has [O III] λλ5007, 4959 line profiles that are very nearly rectangular in shape (on our 5 Å resolution scans) with FWHM of 1050 ± 150 km s^{-1}. Furthermore, the centroids of these lines are within −50 km s^{-1} of the position suggested by the laboratory wavelengths. This contrasts with the more nearly Gaussian shapes of Hα, [N II], and [O II] lines, which have FWHM of 350 ± 75 km s^{-1}. However, the Hα and [N II] lines do show some velocity structure, but below the half-intensity level. This suggests that the additional gas responsible for the [O III] line profiles is of higher ionization than that responsible for the other lines.

A high-dispersion scan of NGC 5005 reveals that it also has multiple emission-line components. In this case, velocity structure is seen throughout the Hα + [N II] blend, the [S II] lines, and in [O I] λ6300. Unfortunately, no further information was obtained because of noise in the scan and the lack of a suitable zero-velocity reference point.

Broad Hα components.—Mrk 883 has weak but noticeable emission extending from the Hα + [N II] blend. This confirms the observations reported by Afanas'ev *et al.* (1980). Since the forbidden lines have full width at zero intensity (FWZI) of about 1500 km s^{-1} (found from the [O I] and [S II] lines) and the FWZI of the Hα + [N II] blend is 3850 ± 600 km s^{-1}, the implied FWZI of Hα is 3850 km s^{-1}. Using either the [O III] λ5007 line or the [S II] λ6716 line to deblend Hα, an estimate could be obtained of the broad-line flux to narrow-line flux ratio. An average of several such subtractions yielded a ratio Hα broad/Hα narrow = 0.43, which translates into a broad-

TABLE 2—*Continued*

Line	Mrk 833	NGC 5005	Mrk 1158	UM 213	Akn 160	Mrk 739	Kaz 26	UM 71	UM 60	Akn 179[a]	Akn 145[a]
O III λ3133.....											
He II λ3204											
[Ne V] λ3346.....											
[Ne V] λ3426.....											
O III λ3444											
[O II] λ3727.....	0.75	5.53	0.69		2.02	1.39:	2.73				
[Ne III] λ3869	0.10	0.29:	0.042		≤0.18	0.044:	0.11				
He I + H8 λ3889.	0.020:	≤0.082	0.011:		...	...	0.063:				
[Ne III] λ3967	0.025:	≤0.21	0.015:		...	...	0.044:				
[S II] λ4071	0.036:	≤0.037	0.007:		...	0.032:	0.039:				
Hδ	0.042	...	0.055		...	0.021:	0.28				
Hγ.....	0.10	...	0.15		...	0.12:	0.83				
[O III] λ4363	0.028	≤0.11	≤0.002		≤0.049	≤0.074	≤0.10				
He II λ4686	0.013	≤0.045	≤0.004	≤0.026	≤0.045	...	≤0.10	≤0.42	...	...	...
Hβ	0.35	0.33	0.42	0.47	0.55	0.86	2.56	3.80	3.98	0.077:	≤0.011
[O III] λ4959	0.31	0.38	0.32	0.34	0.36	0.34	0.30	0.37	0.36	...	...
[O III] λ5007	1.00	1.00	1.00	1.00	1.00	1.00	1.00	1.00	1.00	≤0.017[a]	≤0.014[a]
[Fe VII] λ5159....	...	...	...	...	...	...	...	...	...	...	...
[N I] λ5199	0.013	0.67	≤0.003	0.020	...	0.064:	0.068	...	0.22:	...	...
[Ca V] λ5309.....	...	...	...	...	...	...	...	...	...	...	...
[Fe VII] λ5721....	...	...	...	...	...	...	≤0.011	...	...	...	...
[N II] λ5755.....	≤0.003	...	...	...	...	...	≤0.016	...	≤0.040	≤0.018	...
He I λ5876	0.040	0.35	0.081	0.081	0.097:	0.13	0.35	0.73	0.48	≤0.041	0.033:
[Fe VII] λ6087....	≤0.005	...	...	...	...	...	≤0.020	...	...	...	...
[O I] λ6300	0.18	1.41	0.013	0.070	0.12:	0.37	0.12	0.39	0.53	≤0.010	≤0.002
[S III] λ6312.....	0.009	...	0.003	0.030	...		0.008:	...	...	...	...
[O I] λ6364	0.032	0.44	0.005	0.017	0.10:	0.11	0.064:	0.087	...	...	...
[Fe X] λ6374	...	...	...	...	...	...	...	...	...	...	...
[N II] λ6548.....	0.23	6.38	0.13	0.22	0.48	1.45	2.05	2.82	4.11	0.12	0.15
Hα	1.55 N[b]	4.60	1.88	2.49	4.28	7.32	10.6	25.0	26.4	1.00[a]	1.00[a]
	0.67 B[b]										
[N II] λ6583.....	0.73	19.1	0.40	0.67	1.40	4.28	5.59	9.97	11.9	0.39	0.43
[S II] λ6716	0.40	4.59:	0.18	0.30	1.13	1.10	1.17	4.79	3.58	0.13	≤0.023
[S II] λ6730	0.34	5.06:	0.14	0.25	0.87	1.05	1.14	3.25	2.42	0.16	
F λ5007[c]	6.7(−14)	7.5(−15)	8.7(−13)	2.5(−14)	3.7(−15)	4.2(−15)	6.7(−14)	8.0(−16)	9.6(−16)	6.0(−15)[d]	9.3(−15)[d]
F λ4800[e]	6.7(−27)	7.7(−26)	1.2(−26)	4.2(−27)	3.4(−27)	8.4(−27)	6.7(−26)	4.2(−27)	6.7(−27)	2.2(−27)	9.0(−27)
z.....	0.03794	0.00320	0.01506	0.04058	0.01904	0.02955	0.01360	0.04079	0.03743	0.02899	0.0275

[a] Measurements relative to Hα.
[b] Separate measurements for broad and narrow components.
[c] erg s^{-1} cm^{-2}.
[d] Hα flux in erg s^{-1} cm^{-2}.
[e] erg s^{-1} cm^{-2} Hz^{-1}.

line flux of 4.5×10^{-14} ergs s^{-1} cm^{-2}. Assuming no reddening correction, and with $H_0 = 75$ km s^{-1} Mpc^{-1}, a luminosity of about 1.2×10^{41} ergs s^{-1} is obtained, which is comparable to the values found by Osterbrock (1981) for Seyfert 1.9 galaxies. Finally, no broad Hβ was found in Mrk 883.

As mentioned earlier, our scans (Fig. 1) show that M81 also has a broad Hα component, confirming the discovery made by Peimbert and Torres-Peimbert (1981). For this galaxy, the FWZI of Hα was measured to be 3600 ± 600 km s^{-1}, contrasted with a FWZI of about 1400 ± 300 km s^{-1} for the [S II] lines. The value found by Peimbert and Torres-Peimbert for the FWZI of Hα is 5300 km s^{-1}, which, considering the inaccuracies in measurements of this type, compares favorably with the present result. Using a procedure similar to that used for Mrk 883, the Hα complex was deblended into broad and narrow components, with the results given in Table 3. Again with no reddening correction and assuming $H_0 = 75$ kms^{-1} Mpc^{-1}, a luminosity of approximately 9.2×10^{37} ergs s^{-1} was found for the broad component, which is considerably below L(Hα broad) of other Seyfert 1, 1.5, and 1.9 galaxies. In addition, these observations also confirm the broad [O I] λ6300 line in M81 reported by Heckman, Balick, and Crane (1980) and by Peimbert and Torres-Peimbert (1981). However, because of the heavy underlying stellar absorption, no separation into a broad and a narrow component was possible. Contrary to Peimbert and Torres-Peimbert's results, we did not observe any broad component of Hβ.

e) Continuum Properties

The continuum properties of all but two objects are listed in a previous paper by Shuder (1981). In the present paper, the corresponding continuum fluxes are given as well as the properties of two galaxies not reported on in

TABLE 3

REDDENING-CORRECTED LINE INTENSITY RATIOS

Line	MCG 6-30-15	Akn 347	UM 16	Mrk 533	NGC 6251	I Zw 92	Mrk 612	Mrk 463 E	Mrk 622	Mrk 463 W	M 81
O III λ3133		0.043:	...			0.014					
He II λ3204		0.017:	0.013:			0.006					
[Ne V] λ3426		0.048	0.036			0.029					
[Ne V] λ3426		0.14	0.095			0.082					
O III λ3444		≤0.004	0.019			0.004			0.92		
[O II] λ3727	≤1.88	0.18	0.22	0.18	0.14:	0.26	0.21	0.34	1.98	1.06	3.58
[Ne III] λ3869	≤0.35	0.093	0.13	0.15	...	0.12	0.10	0.10	0.22	0.13	0.41:
He I + H8 λ3889	...	0.020	0.020	0.019	...	0.022	0.014	0.020	...	0.030	...
[Ne III] λ3967	...	0.016	0.040	0.042	...	0.042	0.020	0.038	...	0.007	≤0.063
[S II] λ4071	≤0.019	0.009:	0.012	0.017	...	0.024	0.007	0.023	≤0.051	0.010:	≤0.37
Hδ	...	0.012:	0.018	0.014	...	0.023	0.010	0.026	...	0.014:	≤0.075
Hγ	0.023:	0.036	0.034	0.038	≤0.047	0.054	0.051	0.055	0.033:	0.074	≤0.14
[O III] λ4363	≤0.022	0.028	0.018	0.014	≤0.13	0.035	0.022	0.017	0.009	≤0.033	...
He II λ4686	≤0.085	0.022	0.027	0.027	...	0.015	0.032	0.017	0.037	0.038	...
Hβ	0.063:	0.066	0.072	0.085	0.098:	0.099	0.11	0.14	0.19	0.22	0.35
[O III] λ4959	0.29	0.33	0.33	0.33	0.32	0.35	0.32	0.33	0.35	0.29	0.41
[O III] λ5007	1.00	1.00	1.00	1.00	1.00	1.00	1.00	1.00	1.00	1.00	1.00
[Fe VII] λ5159	...	≤0.003	0.009	0.002	...	0.003	≤0.004	≤0.003	≤0.003	...	...
[N I] λ5199	0.017:	0.005:	0.004	0.004:	0.026:	0.002	0.011	0.011	0.018	0.030:	0.061:
[Ca V] λ5309	...	0.006:	0.001	≤0.001	...	0.001	0.003	0.004:	...	0.003:	...
[Fe VII] λ5721	...	0.008	0.005	0.003	...	0.004	≤0.003	...	≤0.004	...	...
[N II] λ5755	0.009	≤0.002	≤0.001	0.001	0.016	0.002	0.005	≤0.001	≤0.002	...	≤0.008
He I λ5876	0.021	0.008	0.013	0.009	0.003:	0.009	0.022	0.011	0.009	0.010	≤0.033
[Fe VII] λ6087	≤0.001	0.009	0.012	0.005	...	0.007	≤0.002	0.002:	≤0.004	...	...
[O I] λ6300	0.028	0.024	0.019	0.017	0.085	0.049	0.024	0.037	0.041	0.028	0.55
[S III] λ6312	...	...	...	...	...	...	0.004	...	0.011	0.009	...
[O I] λ6364	0.012:	0.004:	0.006	0.008	0.015	0.012	0.004	0.013	0.013	0.005	0.14
[Fe X] λ6374	...	...	...	...	...	≤0.001	...	...	...	...	...
[N II] λ6548	0.080	0.095	0.044	0.060	0.27	0.034	0.14	0.045	0.17	0.086	0.65
Hα	0.16	0.21	0.20	0.18	0.30	0.28	0.31	0.30	0.53	0.48	1.00 N[a]
											1.49 B[a]
[N II] λ6583	0.24	0.26	0.12	0.18	0.79	0.10	0.42	0.14	0.49	0.25	1.82
[S II] λ6716	0.058	0.062	0.034	0.026	0.039	0.041	0.086	0.060	0.084	0.098	0.36
[S II] λ6730	0.056	0.059	0.035	0.030	0.043	0.044	0.063	0.055	0.090	0.082	0.43
E(B–V)	1.7	0.56	0.50	0.71	1.5	0.26	0.61	0.48	1.33	0.93	0.90
	±0.4	±0.12	±0.06	±0.20	±0.6	±0.10	±0.06	±0.13	±0.40	±0.11	±0.4

[a] Separate measurements for broad and narrow components.

that paper. These galaxies are Mrk 739 and Mrk 1158 which, like Kaz 26 and Akn 160, have very blue continua, an absence of high ionization lines such as He II λ4686, and narrow-line profiles (see § V). It may be that these four galaxies contain enough hot stars to produce the photoionization responsible for their emission lines.

IV. ADDITIONAL SPECTRA

In addition to the objects measured and listed in Table 3 or in Koski (1978), spectra of many additional radio-quiet or radio-weak galaxies known or suspected to have emission lines have been taken in the Lick survey. Qualitative descriptions of the spectra of these objects, based on visual inspection of the scans, are listed in Table 6. All Seyfert 1 galaxies are omitted from the table, but all Seyfert 2 galaxies and narrow emission-line galaxies for which we have spectral information not previously published are included. The redshifts of these galaxies (in the reference system of the Sun), measured directly from tracings of the scans and having on the average probable errors of about ±0.0003, are also listed for these galaxies. Three other galaxies, suspected from previous surveys to have emission lines in their spectra, showed no such lines on the Lick scans. Two of these, Akn 206 and Akn 318, have well developed absorption-line spectra with $z = 0.0205$ and 0.0222, respectively; the third, Akn 324, shows no easily identifiable absorption lines on the single rather noisy scan of the red spectral region we have.

V. DISCUSSION

There have been several recent attempts to develop a classification scheme for distinguishing the energy-input mechanism in Seyfert galaxies and in developing a scheme for classifying the Seyfert phenomenon. Following Baldwin, Phillips, and Terlevich (1981), the [O III] λ5007/[O II] λ3727 ratio is plotted in Figure 2 versus the [O III] λ5007/Hβ ratio for galaxies with narrow permitted emission lines. The data are Lick Observatory measurements (Koski 1978; Costero and Osterbrock 1977; Cohen and Osterbrock 1981; and those from the present paper) and have been corrected for the effects of interstellar extinction. Figure 2 clearly shows a cutoff below which λ5007 is consistently weak compared to λ3727. This break occurs at [O III] λ5007/Hβ = 3 to 4. Furthermore, a similar break occurs in an He II λ4686/Hβ versus [O III] λ5007/Hβ diagram, such as that published by Koski

TABLE 3—*Continued*

Line	Mrk 883	NGC 5005	Mrk 1158	UM 213	Akn 160	Mrk 739	Kaz 26	UM 71	UM 60	Akn 179[a]
O III λ3133										
He II λ3204										
[Ne V] λ3346										
[Ne V] λ3426										
O III λ3444										
[O II] λ3727	1.51	26.5	1.26		5.45	5.98:	4.42			
[Ne III] λ3869	0.19	1.16:	0.072		0.44	0.16:	0.17			
He I + H8 λ3889	0.037:	≤0.32	0.019:		...	...	0.096:			
[Ne III] λ3967	0.044:	≤0.77	0.025:		...	...	0.065:			
[S II] λ4071	0.061:	≤0.12	0.011:		...	0.095:	0.056:			
Hδ	0.070	...	0.086		...	0.061:	0.39			
Hγ	0.15	...	0.21		...	0.28:	1.10			
[O III] λ4363	0.042	≤0.25	≤0.003		≤0.086	≤0.17	≤0.13			
He II λ4686	0.016	≤0.068	≤0.005	≤0.030	≤0.058	...	≤0.12	≤0.52	...	...
Hβ	0.38	0.39	0.45	0.55	0.61	1.01	2.70	4.18	4.39	0.34:
[O III] λ4959	0.31	0.40	0.32	0.34	0.37	0.36	0.31	0.38	0.37	...
[O III] λ5007	1.00	1.00	1.00	1.00	1.00	1.00	1.00	1.00	1.00	≤0.064[a]
[Fe VII] λ5159	...	...	...	...	...	...	...	...	...	...
[N I] λ5199	0.012	0.54	≤0.003	0.018	...	0.052:	0.064	...	0.20:	...
[Ca V] λ5309	...	...	...	...	...	...	...	...	...	...
[Fe VII] λ5721	...	...	...	...	...	...	≤0.009	...	...	...
[N II] λ5755	≤0.002	...	...	...	...	...	≤0.013	...	≤0.026	≤0.033
He I λ5876	0.027	0.14	0.057	0.057	0.055:	0.058	0.27	0.46	0.30	≤0.067
[Fe VII] λ6087	≤0.003	...	...	...	...	...	≤0.014	...	...	...
[O I] λ6300	0.10	0.41	0.008	0.043	0.055:	0.12	0.082	0.21	0.28	≤0.012
[S III] λ6312	0.005	...	0.002	0.019	...		0.005:	...	...	...
[O I] λ6364	0.018	0.12	0.003	0.010	0.046:	0.033	0.043:	0.046	...	...
[Fe X] λ6374	...	...	...	...	...	...	...	...	...	...
[N II] λ6548	0.12	1.56	0.077	0.13	0.19	0.39	1.33	1.36	1.95	0.12
Hα	0.82 N[b]	1.11	1.08	1.43	1.74	1.95	6.87	12.0	12.5	1.00[a]
	0.35 B[b]									
[N II] λ6583	0.39	4.55	0.23	0.38	0.56	1.12	3.59	4.74	5.61	0.39
[S II] λ6716	0.20	1.00:	0.099	0.17	0.43	0.27	0.73	2.17	1.61	0.12
[S II] λ6730	0.17	1.09:	0.079	0.14	0.33	0.25	0.71	1.47	1.08	0.15
E(B–V)	0.67	1.5:	0.59	0.58	0.95	1.40	0.46	0.78	0.79	1.4:
	±0.16		±0.14	±0.20	±0.3	±0.35	±0.11	±0.3	±0.3	

[a] Measurements relative to Hα.
[b] Separate measurements for broad and narrow components.

(1978), at [O III]/Hβ ≈ 3. This is strongly suggestive, under the assumption of photoionization, that an increase in the number of high-energy photons is responsible for the increased intensity of He II λ4686 and [O III] λ5007 relative to Hβ. Such an increase can occur if photoionization by a power-law input spectrum, rather than by hot stars, is chiefly responsible for the ionization in galaxies with [O III] λ5007/Hβ ≳ 3.

Using this ratio as a discriminator, possible differences in the physical conditions between the two groups of galaxies, with [O III] λ5007/Hβ ≥ 3 and [O III] λ5007/Hβ < 3, were investigated. Histograms of the temperature-sensitive [O III] line ratio and the density-sensitive [S II] line ratio revealed no significant differences between the two groups. However, shown in Figure 3 is a histogram of emission-line widths for galaxies separated according to their [O III] λ5007/Hβ ratios. The data were taken from the sources mentioned earlier. The four galaxies listed in Table 5, with only upper limits measured for their FWHM, were assigned widths corresponding to that limit. This actually had little bearing on the outcome, since these limits were all below 250 km s^{-1} and occurred in galaxies with small [O III] λ5007/Hβ. Clearly evident is the distinction between the two groups. A galaxy that has [O III] λ5007/Hβ < 3 has FWHM = 310 ± 47 km s^{-1}, while one with [O III] λ5007/Hβ ≥ 3 has FWHM = 550 ± 40 km s^{-1}. Using the *t*-test, a level of significance of less than 0.001 (*t* statistic = 3.61 and 48 degrees of freedom) is found for the hypothesis that there is essentially no difference between the two sample means. Thus, these groups are apparently from different parent distributions. *Consequently, an* [O III] λ*5007*/Hβ *ratio* ≥ 3 *seems a good basis for defining the Seyfert phenomenon among the Seyfert 2 and other narrow-line galaxies.* However, because Figure 3 shows that some overlap in line widths exists between the two groups, an additional criterion might be FWHM ≥ 300 km s^{-1}. This would also avoid confusion with the H II region–like galaxies described by Sargent and Searle (1970), French (1980), and others, which have very narrow lines, but some of which have [O III] λ5007/Hβ ≥ 3. They all have weak He II λ4686 (or none at all), and are almost certainly photoionized by hot main-sequence stars.

Other correlations of line widths with emission proper-

TABLE 4

ESTIMATES OF DENSITY AND TEMPERATURE

Object	O III Zone	N II + S II Zone	
	Temperature (K) (Ne → 0)	Temperature (K)	Density (cm^{-3})
MCG 6-30-15	≤15800	15700	850
Akn 347	17400	8900	630
UM 16	14200	7900	2000
Mrk 533	12800	...	1150[a]
NGC 6251	...	11000	1050
I Zw 92	19600	15000	2200
Mrk 612	15500	8500	80
Mrk 463 E	13800	10000	1500
Mrk 622	10900	≤6450	800
Mrk 463 W	≤19500	7100	300
M81	...	≤7600	≤1500
Mrk 833	22500	≤7000	≤270
NGC 5005	...	7000	900
Mrk 1158	≤8000	≤8000	200[b]
UM 213	...	...	300[a]
Akn 160	≤41000	...	150[a]
Mrk 739	...	...	550[a]
Kaz 26	...	6600	660
UM 71	...	...	≤100
UM 60	...	≤6700	≤100
Akn 179	...	...	1400[a]
Akn 145	...	...	...

[a] Density given at a temperature of 10,000 K.
[b] Density given at a temperature of 8000 K.

ties of galaxies were noted by Wilson and Willis (1980) and Weedman *et al.* (1980). These investigators found that the line widths appeared to be correlated with the radio luminosities and with the infrared excesses. The quantitative definitions we have adopted above thus seem well suited to isolate galaxies with nonthermal activity in their nuclei and have the added benefit of being conveniently observable.

With the above definition of a Seyfert 2 galaxy (i.e., [O III] λ5007/H$\beta \geq 3$ and FWHM ≥ 300 km s^{-1}), the Seyfert 2 galaxies in Table 3 are MCG 6-30-15, Akn 347, UM 16, Mrk 533, NGC 6251, I Zw 92, Mark 612, Mrk 463 E, Mrk 622, and Mrk 463 W. The galaxies that probably are not Seyfert 2 galaxies are M81, Mrk 883 (although these two objects might be weak examples of Seyfert 1.9 galaxies), and NGC 5005 (which may have a weak nonthermal continuum). Galaxies that are not Seyfert 2 galaxies are Mrk 1158, UM 213, Akn 160, Mrk 739, Kaz 26, UM 71, UM 60, Akn 179, and Akn 145. In addition,

TABLE 5

EMISSION-LINE FWHM (km s^{-1})

Object	Width
MCG 6-30-15	300 ± 100
Akn 347	325 ± 75
UM 16	375 ± 75
Mrk 533	550 ± 50
NGC 6251	625:
I Zw 92	400 ± 100
Mrk 612	375 ± 75
Mrk 463 E	700 ± 100
Mrk 622	350 ± 75
Mrk 463 W	475 ± 75
M81	325 ± 100
Mrk 883	325 ± 100
NGC 5005	775 ± 100
Mrk 1158	≤250
UM 213	≤175
Akn 160	175 ± 50
Mrk 739	200 ± 100
Kaz 26	≤250
UM 71	≤150
UM 60	225 ± 75
Akn 179	225 ± 75
Akn 145	175:

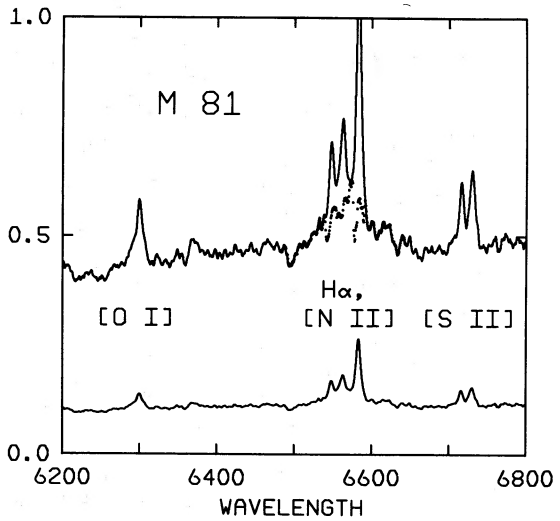

FIG. 1.—A portion of a high dispersion scan for M81, plotted at two scale factors. The ordinate is relative energy per unit Å, while the abscissa is rest wavelength in Å. The top scan also shows the residual intensity after removal of [N II] and Hα.

TABLE 6

ADDITIONAL SPECTRA OF SEYFERT 2 AND EMISSION-LINE GALAXIES

Object	z	Estimated Line Ratios [O III] λ5007 / Hβ	[O I] λ6300 / Hα	[S II][a] / Hα	[N II] λ6583 / Hα	Other Lines	Line Widths[b]	Remarks
NGC 6500	0.0107	1.5	0.25	0.7	0.75	[O II]	≈	Not Sey 2
Mrk 391	0.0140	--	0.08	0.2			≈	Not Sey 2[c]
Mrk 442	0.0147	c	≳2.0	≳2.0	≳2.0		≈	Not Sey 2[c]
Mrk 446	0.0232	≲0.5	≲0.02	0.08	0.8		≈	Not Sey 2[c]
Mrk 610	0.0350	<0.2	0.04	0.15	0.4		≈	Not Sey 2
Mrk 688	0.0393	0.6	0.03	0.2	0.3	[O II]	≈	Not Sey 2
Mrk 789	0.0333	0.9	0.01	0.1	0.3	He I	≈	Not Sey 2
Mrk 1308	0.0041	0.8	≲0.01	0.1	0.25	[O II]	≈	Not Sey 2
Mrk 1344	0.0120	2.7	0.05	0.15	0.4	He I	≈	Not Sey 2 ?
II Zw 4	0.0136	3	~0.01	0.1		[O II], [Ne III], He I	≈	II Zw 40[c]
II Zw 23	0.0277	1.5	~0.04	0.15		[O II], He I	≈	II Zw 40[c]
II Zw 23 comp	0.0284	1.2	~0.02	~0.1		[O II], He I		
Akn 79	0.0170	6	0.2	0.8		[O II]	≥	Sey 2 ?
Akn 80	0.0341	<0.3		0.1	0.33		≈	Not Sey 2
Akn 129	0.0166	c	≲0.07	0.25	0.5		≈	Not Sey 2[c]
Akn 131	0.0278	≲1		≲0.06	0.3		≈	Not Sey 2
Akn 140	0.0149	c	≲0.05	0.15	0.4		≈	Not Sey 2[c]
Akn 151	0.0404	0.3	0.03	0.15	0.5		≈	Not Sey 2
Akn 170	0.0229	c	≲0.1	≲0.1	0.5		≈	Not Sey 2[c]
Akn 179	0.0298	c	≲0.1	0.2	0.4		≈	Not Sey 2[c]
Akn 223	0.0220	c	≲0.2	0.6	≲0.2		≈	Not Sey 2[c]
Akn 232	0.0268	1.2	≲0.03	0.1	0.5		≈	Not Sey 2
Akn 253	0.0266	0.6	0.03	0.1	0.4	[O II], [N I], He I	≈	Not Sey 2
Akn 402	0.0183	c	0.3	2	2		>	c
Akn 481	0.0259	c	≲0.07	<0.1	0.6		≈	Not Sey 2
Akn 539	0.0169	15	0.2	0.5	0.6	[O II]	≈	Sey 2
UM 90	0.0179	c	≲0.2	0.8	1.5		≈	Not Sey 2[c]
UM 93	0.0316	≲0.1	0.02	0.1	0.5		≈	Not Sey 2
UM 135	0.0181	c	0.03	0.15	0.4		≈	Not Sey 2
UM 246	0.0600	10	0.1	0.25	0.6		≈	Sey 2
M 51	0.0014	c	0.15	0.5			≈	Not Sey 2[c]

[a] Average strength of [S II] λ6716+λ6730 relative to Hα.
[b] In line width column ≈ means line width ≈ instrumental resolution (500 km s^{-1}) and > means line width > instrumental resolution.
[c] Additional remarks below.

REMARKS TO TABLE 6

Mrk 391: Hβ undetectable; [O III] λ5007 present but very weak.
Mrk 442: = NGC 4687. Hα not visible, only weak [O I], [N II], [S II] visible. Redshift from emission and absorption lines.
Mrk 446: Hβ very weak but dectable.
II Zw 4: Similar to II Zw 40 described by French 1980.
II Zw 23: Similar to II Zw 40 described by French 1980.
Akn 129: Have no blue scan. [O III] λ5007 weak if at all present on red scan.
Akn 140: Have no blue scan. Hβ and [O III] λ5007 weak if at all present on red scan.
Akn 170: Hβ, [O III] λ5007 not visible on rather noisy scan.
Akn 179: Hβ, [O III] λ5007 not visible on rather noisy scan.
Akn 223: Hβ, [O III] λ5007 not visible on rather noisy scan.
Akn 402: Hβ, [O III] λ5007 not visible. All emission lines very weak. Deserves further study.
Akn 481: Hβ, [O III] not visible.
UM 90: Hβ, [O III] not visible.
UM 135: Have no good blue scan.
M51: Strong absorption Hβ; no emission Hβ seen but no doubt has disappeared in absorption line.

the objects listed by Koski (1978) that are not Seyfert 2 galaxies are I Zw 81, Mrk 298, Mrk 507, Mrk 700, NGC 6764, and Mrk 378. Note that Koski also suspected these sources were not Seyfert 2 galaxies.

We have also explored the differences and similarities between the narrow-line regions of Seyfert 1 galaxies and Seyfert 2 galaxies. Shown in Figures 4 and 5 are histograms of the temperature-sensitive [O III] ratio and the density-sensitive [S II] ratio for broad-permitted-line objects (QSOs, Seyfert 1 galaxies, and broad-line radio galaxies) that have not been corrected for reddening, and narrow-permitted-line objects (Seyfert 2 galaxies, narrow-line radio galaxies, and emission-line galaxies) corrected for reddening. The data came from Baldwin (1975), Osterbrock (1977), Grandi and Osterbrock (1978), Koski (1978), Costero and Osterbrock (1977), Cohen and Osterbrock (1981), and the present paper. As has been noted in the past (Osterbrock 1977, 1978; Heckman and Balick 1979), the [O III] ratio is lower in Seyfert 1 galaxies than in Seyfert 2 galaxies, while the

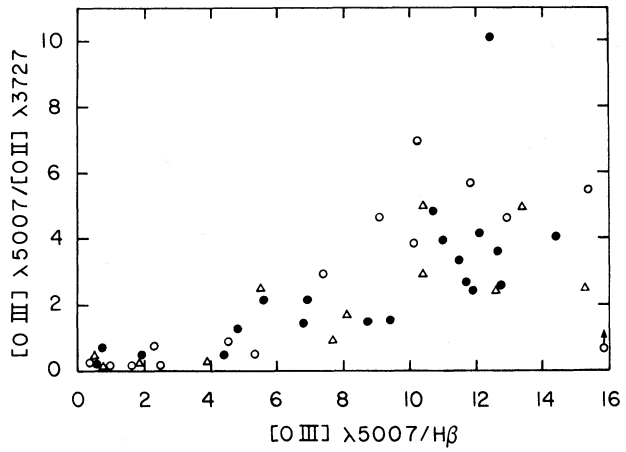

FIG. 2.—Corrected line-intensity ratios are presented for narrow-line radio galaxies (*triangles*), for emission-line galaxies measured by Koski (1978) (*solid circles*), and for galaxies measured in this paper (*open circles*).

[S II] line ratios are very nearly equal. This is very nicely demonstrated in the present paper (Figs. 4 and 5) from which it is found that the average [O III] ratio for the broad-permitted-line objects is 29 ± 3.4, while for the narrow-permitted-line objects it is 53 ± 4.9. Using a Student's *t*-test, a level of significance of 0.998 is determined for the hypothesis that the two groups arise from different parent distributions. The possibility exists that the strength of [O III] λ4363 is systematically overestimated in Seyfert 1 galaxies because of blending with the much stronger Hγ line. Visual inspection of our scans, however, shows that several galaxies having a clearly identifiable peak at λ4363 also have a low [O III] ratio. Consequently, it seems to us that this is an intrinisic property of Seyfert 1 galaxies.

Yee (1980) and Shuder (1981) showed that the luminosities of the H I and He II emission lines in Seyfert 1 and Seyfert 2 galaxies are well correlated with the continuum luminosities, so long as the total (broad-line plus narrow-line components) profiles are measured. This correlation holds over a very wide range of luminosities and extends to QSOs. The forbidden lines, however, were shown to have larger luminosities in Seyfert 2 galaxies than in Seyfert 1 galaxies, for a given continuum luminosity. To investigate this point further, as well as the fact that

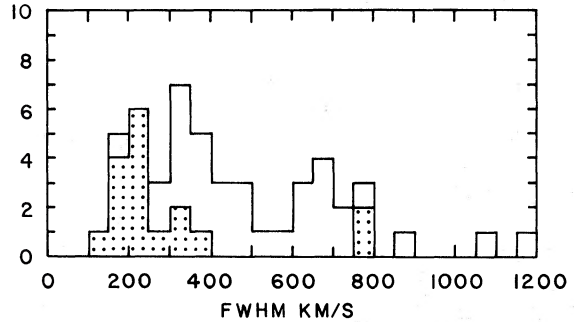

FIG. 3.—Histogram of emission-line widths for galaxies with [O III] λ5007/Hβ < 3 (*dotted areas*), and for galaxies with [O III] λ5007/Hβ > 3 (*open areas*).

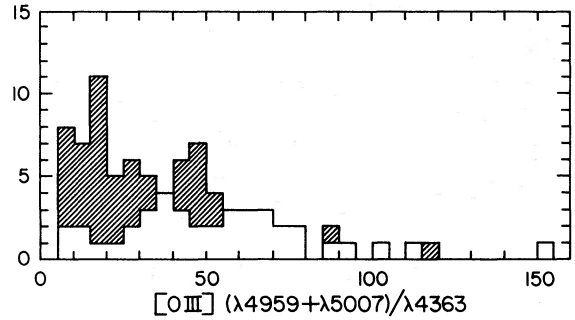

FIG. 4.—Histogram of the temperature-sensitive [O III] (λ4959 + λ5007)/λ4363 line ratio for emission-line galaxies, narrow-line radio galaxies, and Seyfert 2 galaxies (*open areas*), and for broad-line radio galaxies, Seyfert 1 galaxies, and QSOs (*hatched areas*).

[Fe VII] λ6087 appears stronger on the average in Seyfert 1 than in Seyfert 2 galaxies (Heckman and Balick 1979; Cohen 1980), a plot was made of the luminosity of this line as a function of the luminosity of the featureless continuum at λ4800. The luminosities are corrected for the effects of galactic extinction using the cosecant law of Burstein and McDonald (1975). As Figure 6 shows, the luminosity of [Fe VII] λ6087 in Seyfert 1 galaxies is not suppressed relative to the luminosity of the same line in Seyfert 2 galaxies.

One possible interpretation of the greater strength of [Fe VII] in Seyfert 1 galaxies is that the photoionizing power-law continuum may simply extend to higher energies in Seyfert 1 galaxies than in Seyfert 2 galaxies. Photons with energy $h\nu \geq 103$ eV are required to ionize Fe^{+5} to Fe^{+6}, the ion which emits the [Fe VII] spectrum. There is a very clear correlation between the strength of the featureless continuum in the optical region and presence or absence of broad emission lines (Osterbrock 1980). There may also be a correlation between the upper limit of energy to which the power-law spectrum extends and the presence or absence of broad emission lines. If this is the correct interpretation, then [Ne V], which requires ionizing photons with $h\nu \geq 97$ eV, would also be expected to be strengthened relative to the low-ionization lines in Seyfert 1 galaxies.

Another possibility is the model introduced by Osterbrock (1978), in which the forbidden-line region is ionized

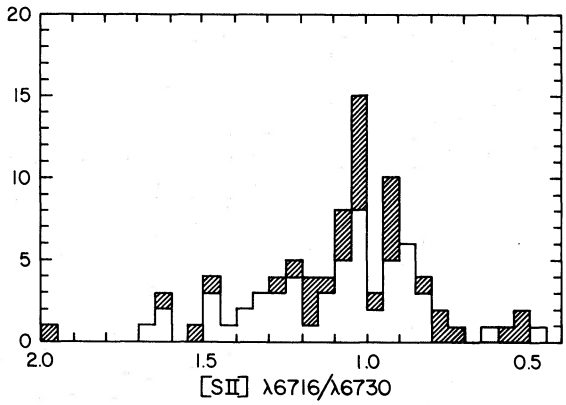

FIG. 5.—Same as in Fig. 4, but for [S II] λ6716/λ6730

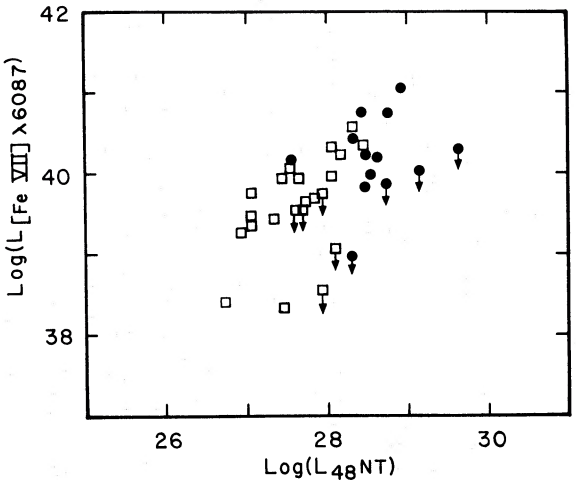

FIG. 6.—The log of the [Fe VII] λ6087 luminosity in ergs s^{-1} vs. the log of the nonthermal continuum luminosity at λ4800 in ergs s^{-1} Hz^{-1}, corrected for extinction within our Galaxy. Plotted are Seyfert 1 galaxies (*circles*), and narrow-line radio galaxies and Seyfert 2 galaxies (*squares*).

by continuum radiation that has passed through holes, channels, or gaps in the dense broad-line region. Under this hypothesis, the [Fe VII] lines would be produced near the broad-line zone where the flux of ionizing photons is largest. An immediate problem is the lack of observations showing broad [Fe VII] lines. Recently, however, Wilson (1979) has reported that the high-ionization lines are indeed broader than the lower-ionization lines in the Seyfert 1 galaxy NGC 3783, although not as broad as the permitted lines, and Osterbrock (1981) has found the same result in III Zw 77. Moreover, Cohen (private communication) has found that the [Fe X] λ6374 line in the Seyfert 1.5 galaxy Mrk 975 is significantly broader than the other forbidden lines. Thus, there are several indications that the high-ionization lines are produced close to, though usually not within, the broad-line region.

VI. CONCLUSIONS

The results of the present study of Seyfert 2 and emission-line galaxies, combined with previous Lick Observatory data, form a large homogeneous data base for investigations of active nuclei. We have found that a quantitative association appears to exist between the emission-line FWHM and the [O III] λ5007/Hβ ratio in narrow-line galaxies. This association links ratios of [O III] λ5007/Hβ < 3, with lines having FWHM < 300 to 400 km s^{-1}. For larger [O III] λ5007/Hβ, the spectra also show greater He II λ4686/Hβ ratios, and the emission lines also have FWHM > 300 km s^{-1}. These criteria form a good quantitative basis for distinguishing the Seyfert 2 galaxies from other emission-line galaxies.

We have also demonstrated that [Fe VII] λ6087 is stronger, relative to the low-ionization lines, in Seyfert 1 galaxies than in Seyfert 2 galaxies. We suggest that in future measurements of Seyfert galaxies particular attention be paid to high-ionization lines such as [Ne V] and [Fe X], which may show similar results.

We are very grateful to G. Kojoian and D. F. Dickinson for communicating to us a list of galaxies which they observed for weak radio emission, and to M. Arakelian for communicating a list of suspected emission-line galaxies. We would also like to thank R. D. Cohen for many useful discussions. We are most grateful to the National Science Foundation for their continued support of this research, most recently under grant AST 79-19227.

REFERENCES

Afanas'ev, V. L., Lipovetskii, V. A., Markaryan, B. E., and Stepanyan, Dzh. A. 1980, *Astrofizika*, **16**, 193.
Baldwin, J. A. 1975, *Ap. J.*, **201**, 26.
Baldwin, J. A., Phillips, M. M., and Terlevich, R. J. 1981, *Pub. A.S.P.*, **93**, 5.
Brocklehurst, M. 1971, *M.N.R.A.S.*, **153**, 471.
Burstein, D., and McDonald, L. H. 1975, *A.J.*, **80**, 17.
Cohen, R. D. 1980, *Bull. AAS*, **12**, 809.
Cohen, R. D., and Osterbrock, D. E. 1981, *Ap. J.*, **243**, 81.
Costero, R., and Osterbrock, D. E. 1977, *Ap. J.*, **211**, 675.
French, H. B. 1980, *Ap. J.*, **240**, 41.
Grandi, S. A., and Osterbrock, D. E. 1978, *Ap. J.*, **220**, 783.
Hayes, D. S., and Latham, D. W. 1975, *Ap. J.*, **197**, 593.
Heckman, T. M., and Balick, B. 1979, *Astr. Ap.*, **79**, 350.
Heckman, T. M., Balick, B., and Crane, P. C. 1980, preprint.
Humason, M. L., Mayall, N. U., and Sandage, A. R. 1956, *A.J.*, **61**, 97.
Kazarian, M. A. 1979, *Astrofizika*, **15**, 17.
Khachikian, E. Y., and Weedman, D. W. 1971, *Astrofizika*, **7**, 389.
———, 1974, *Ap. J.*, **192**, 581.
Koski, A. T. 1976, Ph.D. thesis, University of California, Santa Cruz.
———. 1978, *Ap. J.*, **233**, 56.
Kunth, D., and Sargent, W. L. W. 1979, *Astr. Ap.*, **76**, 50.
MacAlpine, G. M., Lewis, D. W., and Smith, S. B. 1977, *Ap. J. Suppl.*, **35**, 203.
MacAlpine, G. M., Smith, S. B., and Lewis, D. W. 1977*a*, *Ap. J. Suppl.*, **34**, 95.
———. 1977*b*, *Ap. J. Suppl.*, **35**, 197.
Miley, G. K., and Osterbrock, D. E. 1979, *Pub. A.S.P.*, **91**, 257.
Miller, J. S., and Mathews, W. G. 1972, *Ap. J.*, **172**, 593.
Miller, J. S., Robinson, I. B., and Wampler, E. J. 1976, *Advances in Electronics and Electron Physics*, Vol. **40B** (New York: Academic Press), p. 693.
O'Connell, R. W., and Kingham, K. A. 1978, *Pub. A.S.P.*, **90**, 244.
Osterbrock, D. E. 1977, *Ap. J.*, **215**, 733.
———. 1978, *Proc. Nat. Acad. Sci.*, **75**, No. 2, 540.
———. 1980, *Recent Advances in Observational Astronomy: Instrumentation and Results* (Mexico City: UNAM), in press.
———. 1981, preprint.
Peimbert, M., and Torres-Peimbert, S. 1981, *Ap. J.*, **245**, 845.
Phillips, M. M. 1978, *Ap. J. Suppl.*, **38**, 187.
Sargent, W. L. W., and Searle, L. 1970, *Ap. J. (Letters)*, **162**, L155.
Seaton, M. J. 1975, *M.N.R.A.S.*, **170**, 475.
———. 1978, *M.N.R.A.S.*, **185**, 5 p.
Seyfert, C. K. 1943, *Ap. J.*, **97**, 28.
Shuder, J. M. 1981, *Ap. J.*, **244**, 12.
Stone, R. P. S. 1974, *Ap. J.*, **193**, 135.
———. 1977, *Ap. J.*, **218**, 767.
Weedman, D. W. 1977, *Ann. Rev. Astr. Ap.*, **15**, 69.
Weedman, D. W., Balzano, V., Feldman, F., and Ramsey, L. 1980, *Bull. AAS.*, **12**, 504.
Wilson, A. S. 1979, *Proc. Roy. Soc. London A.*, **366**, 461.
Wilson, A. S., and Willis, A. G. 1980, *Ap. J.*, **240**, 429.
Yee, H. K. C. 1980, *Ap. J.*, **241**, 894.

JAMES M. SHUDER and DONALD E. OSTERBROCK: Lick Observatory, University of California, Santa Cruz, CA 95064